Amplitude Adaptive ASDM without Envelope Encoding

Kaspars Ozols
and Rolands Shavelis
Institute of Electronics and Computer Science
14 Dzerbenes Str., LV-1006, Riga, Latvia
Email: kaspars.ozols@edi.lv, shavelis@edi.lv

***Abstract*—In this paper a method of encoding the signals by using Amplitude Adaptive Asynchronous Sigma-Delta modulator (AA-ASDM) scheme without an additional envelope encoding of the signal is proposed. According to AA-ASDM, the time-varying envelope function of the input signal is used in the feedback loop to reduce the switching rate of the output trigger and thus the power consumption of the circuit. In previous work, the signal and its envelope function were encoded and transmitted separately, thus resulting in inefficiency, since two signals instead of one were required to be transmitted. In order to solve this inefficiency, in this paper it is proposed to select such a time-varying envelope function which does not require additional encoding and transmission, and still be able to recover the original signal from the obtained time sequence. The proposed method is particularly advantageous for signals with wide dynamic range.**

I. Introduction

As wireless technologies evolve, more and more new energy constrained sensing applications appear, such as wearables, portable medical devices, wireless sensor networks and others. One of the most important issue in such applications is energy consumption and management of the battery life. In order to deal with this issue, researchers are trying to find new and effective solutions to reduce the power consumption of wireless devices and thus prolong the life of the battery.

One essential part of all wireless sensing devices is an analog to digital converter (ADC), the energy consumption of which can be significantly reduced.

As shown in [1], [2], [3], asynchronous designs, instead of synchronous, in ADCs exhibit better properties such as exclusion of electromagnetic interference, immunity to metastable behaviour, absence of clock jitter and most importantly lower energy consumption.

One such asynchronous ADC is Asynchronous sigma-delta modulator (ASDM), which converts amplitude information into time sequence in a very energy efficient way. The latest implementations show that it is possible to create ASDM with power consumption less than $28nW$ [4]. The fundamentals of ASDM are given in [5].

In previous paper [6], an improved version of ASDM, called Amplitude Adaptive Asynchronous Sigma-Delta modulator (AA-ASDM) was presented, where by using time-varying envelope of the input signal in the feedback loop of ASDM, it was possible to reduce the switching activity of ASDM and thus the power consumption of the circuit by up to 59.86%. Regardless of this reduction the perfect recovery of the original signal from the obtained time sequence was still possible. [6]

However, as concluded in [6], the efficiency of AA-ASDM could still be improved if there was no necessity to additionally encode and transmit the time-varying envelope function of the signal in order to recover it at a receiver.

Further studies have led us to a solution which not only solves the above-mentioned problem, but also further reduces the power consumption of the circuit.

Therefore, in this paper an improved version of AA-ASDM is presented in Section III, which requires the time-varying envelope function of the input signal as proposed in Section IV. The method is particularly advantageous for signals with wide dynamic range, as shown by numerical simulations using electroencephalogram (EEG) signals in Section V.

II. Asynchronous Sigma-Delta Modulator

The block diagram of classical Asynchronous Sigma-Delta modulator (ASDM), which consists of integrator and Schmitt trigger is shown in Fig.1. ASDM circuit is defined by κ, δ and b parameters, which determine the average switching rate of the Schmitt trigger and thus the energy consumption of the circuit. [7]

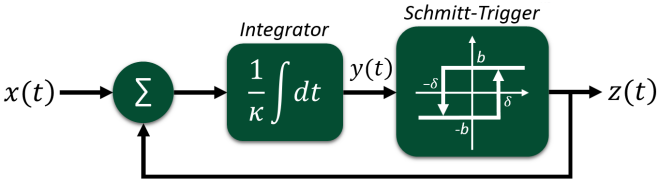

Fig. 1. ASDM block diagram.

The input signal $x(t)$ is bounded in amplitude as

$$|x(t)| \leq c < b \tag{1}$$

Since output of the Schmitt trigger has either $z(t) = -b$ or $z(t) = b$ value, the integrator input is either $x(t)-b$ or $x(t)+b$. By considering (1), it follows that the integrator output $y(t)$ is increasing or decreasing function for $t \in [t_k, t_{k+1}]$, thus $y(t_k) = (-1)^k\delta$ and

$$\int_{t_k}^{t_{k+1}} x(t)dt = (-1)^k[2\kappa\delta - b(t_{k+1} - t_k)] \tag{2}$$

978-0-9928-6265-7/16/$31.00 ©2016 IEEE

for all k, where $k \in Z$. [7] The signal from the obtained time sequence can be perfectly reconstructed as described in [7] if

$$\sup_{k\in Z}(t_{k+1} - t_k) \leq \frac{\pi}{\Omega}, \tag{3}$$

where Ω is the bandwidth of the signal.

Due to (1) the distances between consecutive trigger switching points t_k and t_{k+1} are bounded as

$$\tau_{min} = \frac{2\kappa\delta}{b+c} \leq t_{k+1} - t_k \leq \frac{2\kappa\delta}{b-c} = \tau_{max} \tag{4}$$

Assuming that C is a maximum value of $|x(t)|$ and $c(t) \geq |x(t)|$ is a time-varying envelope of the signal, the maximum and minimum distances τ_{max} and τ_{min} are time-varying as well:

$$\tau_{max1}(t) = \frac{2\kappa\delta}{b - c(t)} = \frac{T}{1 + 1/\alpha - c(t)/(\alpha C)} \tag{5}$$

$$\tau_{min1}(t) = \frac{2\kappa\delta}{b + c(t)} = \frac{T}{1 + 1/\alpha + c(t)/(\alpha C)}, \tag{6}$$

where coefficient $\alpha > 0$ and parameters b and δ are chosen as $b = (1+\alpha)C$ and $\delta = \alpha CT/(2\kappa)$. [6]

As shown in [6], if signals with wide dynamic range are encoded, both distances τ_{min1} and τ_{max1} for small $c(t)$ values are considerably less than T and thus over-triggering occurs, which is not necessary for reconstruction of the original signal. This is due to ASDM circuit parameters are chosen considering only the maximum value which is never exceeded by the signal. [6]

Since dynamic power consumption of the trigger is directly proportional to its switching activity, the energy consumption of the whole ASDM circuit reduces, if the average switching rate of the Schmitt trigger decreases. This also leads to a decreased number of time codes needed to be transmitted. The number of triggerings can be reduced, if the coefficient α is increased, however, too high α values lead to small differences $\tau_{max1} - \tau_{min1}$ and thus more precision is needed to encode the distances between consecutive trigger times. [6]

III. Amplitude Adaptive Asynchronous Sigma-Delta Modulator

Since the envelope of the signal changes over time, in [6] it was proposed to change the constant parameter b according to the time-varying maximum value $c(t) \geq |x(t)|$ to ensure

$$\tau_{max2}(t) = \frac{2\kappa\delta_2}{b_2(t) - c(t)} = const. = T. \tag{7}$$

In this case the difference $b_2(t) - c(t)$ must be constant and thus $b_2(t)$ can be written as

$$b_2(t) = c(t) + \beta C, \tag{8}$$

where $\beta > 0$. The second parameter $\delta_2 = \beta CT/(2\kappa)$ follows from (7) and the minimum distance becomes [6]

$$\tau_{min2}(t) = \frac{2\kappa\delta_2}{b_2(t) + c(t)} = \frac{T}{1 + 2c(t)/(\beta C)}. \tag{9}$$

As shown in [6], in this case $\tau_{min2} > \tau_{min1}$ and $\tau_{max2} > \tau_{max1}$ for all $c(t)$ and $\beta = \alpha$ values, which means the over-triggering reduces and the power consumption as well in comparison to the classical $b = const.$ case. Also the differences $\tau_{max2} - \tau_{min2}$ are larger for all $c(t) < C$ values.

The block diagram of the Amplitude Adaptive Asynchronous Sigma-Delta Modulator (AA-ASDM) is shown in Fig.2. In addition to ASDM circuit (Fig. 1) there is an envelope

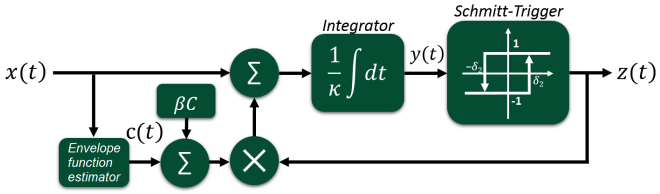

Fig. 2. AA-ASDM block diagram.

detector with output $c(t)$ connected in the feedback loop, therefore now instead of (2) the following equation holds [6]:

$$\int_{t_k}^{t_{k+1}} x(t)dt = (-1)^k[2\kappa\delta - \beta C(t_{k+1} - t_k) - \int_{t_k}^{t_{k+1}} c(t)dt], \tag{10}$$

where κ, δ, β, C are given coefficients.

A method of recovery of the original signal is described in [6], where the envelope function of the signal is also needed for reconstruction of $x(t)$, therefore $c(t)$ is encoded by another ASDM. This is the drawback of AA-ASDM in [6]. In order to increase the efficiency, it is necessary to find such a time-varying envelope function which does not require additional encoding and transmission in order to recover the original signal.

IV. Proposed Method

In order to solve the weak point of AA-ASDM, in this paper it is proposed to choose the time-varying envelope function as follows.

A. Envelope Function

The time-varying envelope can be chosen as:

$$c(t) = const. + x^2(t), \tag{11}$$

where the input signal $x(t)$ is bounded in amplitude: $x(t) \in [-1, 1]$. By choosing $const. = 0.25$, the inequality $c(t) \geq x(t)$ holds for all $x(t) \in [-1, 1]$, therefore the time-varying envelope $c(t)$ of the input signal $x(t)$ is selected as:

$$c(t) = 0.25 + x^2(t) \geq x(t), \tag{12}$$

which does not require any additional encoding scheme (see Section IV-B).

B. Signal Recovery

By inserting (12) into (10), a relationship between the output sequence $\{t_k\}_{k=1,2,\dots,K}$ and the input signal $x(t)$ of AA-ASDM can be obtained:

$$\int_{tk}^{t_{k+1}} x(t) = (-1)^k[2\kappa\delta - \beta C(t_{k+1}-t_k) - \\ - \int_{tk}^{t_{k+1}} (0.25 + x^2(t))dt]. \tag{13}$$

By denoting

$$q_k = (-1)^k[2\kappa\delta - (\beta C + 0.25)(t_{k+1}-t_k)], \tag{14}$$

the equation (13) becomes:

$$\int_{tk}^{t_{k+1}} x(t) + (-1)^k \int_{tk}^{t_{k+1}} x^2(t)dt = q_k. \tag{15}$$

By assuming that the input signal $x(t)$ can be represented as

$$x(t) = \sum_{n=0}^{N-1} d_n g_n(t), \tag{16}$$

where d_n are unknown coefficients and $g_n(t)$ are chosen base functions, the first term of (15) can be written as

$$\int_{tk}^{t_{k+1}} x(t)dt = \sum_{n=0}^{N-1} d_n \int_{tk}^{t_{k+1}} g_n(t)dt = \mathbf{d}^T\mathbf{g}_k, \tag{17}$$

where $\mathbf{d} = [d_0, d_1, \cdots, d_{N-1}]^T$ and

$$\mathbf{g}_k = \begin{bmatrix} \int_{tk}^{t_{k+1}} g_0(t)dt \\ \int_{tk}^{t_{k+1}} g_1(t)dt \\ \vdots \\ \int_{tk}^{t_{k+1}} g_{N-1}(t)dt \end{bmatrix}. \tag{18}$$

The second term of (15) can be written as

$$\int_{tk}^{t_{k+1}} x^2(t)dt = \int_{tk}^{t_{k+1}} \Big(\sum_{n=0}^{N-1} d_n g_n(t)\Big)^2 dt = \\ = \mathbf{d}^T \cdot \hat{\mathbf{G}}_k \cdot \mathbf{d}, \tag{19}$$

where $\hat{\mathbf{G}}_{k_{mn}} = \int_{tk}^{t_{k+1}} g_m(t)g_n(t)dt$. From (15), (17) and (19) the final equation corresponding to the time interval $t \in [t_k, t_{k+1}]$ follows:

$$\mathbf{d}^T \cdot \mathbf{g}_k + (-1)^k \mathbf{d}^T \cdot \hat{\mathbf{G}}_k \cdot \mathbf{d} = q_k. \tag{20}$$

As there are total $K-1$ time intervals, then $K-1$ equations are obtained, and the unknown coefficients $\mathbf{d}$ are found by minimizing the error value:

$$\sum_{k=1}^{K-1} \Big(\mathbf{d}^T \cdot \mathbf{g}_k + (-1)^k \mathbf{d}^T \cdot \hat{\mathbf{G}}_k \cdot \mathbf{d} - q_k\Big)^2. \tag{21}$$

The question is what base functions $g_n(t)$ to choose for representing the input signal $x(t)$, the bandwidth of which is limited to $\omega \in [-\Omega, \Omega]$. The classical answer would be to select $g_n(t) = \text{sinc}(\Omega(t - t_n))$, however, two problems exist: 1) these functions are well suited for representing only time-unlimited signals; 2) calculation of $\mathbf{g}_k$ and $\hat{\mathbf{G}}_k$ is both time consuming and not perfectly precise since no analytical solutions of the integrals exist. Therefere, given the output sequence $\{t_k\}_{k=1,2,\dots,K}$ with the corresponding time period $\Theta = t_K - t_1$, the input signal for $t \in [t_1, t_K]$ is expressed in Fourier series as

$$x(t) = d_0 + \sum_{m=1}^{M} \Big(d_m \cos(m\frac{2\pi}{\Theta}t) + d_{m+M} \sin(m\frac{2\pi}{\Theta}t)\Big), \tag{22}$$

where the upper limit M follows from the bandwidth Ω of the signal:

$$M = \Big\lfloor \frac{\Omega\Theta}{2\pi} \Big\rfloor. \tag{23}$$

Such a representation of $x(t)$ is both well suited for expressing time-limited signals of length Θ and allows fast and precise calculation of $\mathbf{g}_k$ and $\hat{\mathbf{G}}_k$.

C. Real-Time Signal Recovery

In order to reconstruct the signal in real-time, the reconstruction must be carried out in short time intervals $t \in [t_{\gamma J}, t_{\gamma J+L}]$, where $\gamma = 0, 1, 2, \dots$ designates the order number of the interval, but J determines the number of switchings atfer which the reconstruction of the next interval can start [8].

Since the precision of the reconstructed signal fragment at the beginning and at the end of the fragment is low, the reconstructed signal $\hat{x}_\gamma(t)$ is multiplied by a corresponding window function [8] :

$$w_\gamma(t) = \begin{cases} 0, & \text{if} \quad t \notin (\tau_\gamma, \sigma_{\gamma+1}], \\ \theta_\gamma(t), & \text{if} \quad t \in (\tau_\gamma, \sigma_\gamma], \\ 1, & \text{if} \quad t \notin (\sigma_\gamma, \tau_{\gamma+1}], \\ 1 - \theta_{\gamma+1}(t), & \text{if} \quad t \in (\tau_{\gamma+1}, \sigma_{\gamma+1}], \end{cases} \tag{24}$$

where $\tau_\gamma = t_{\gamma J+I}$, $\sigma_\gamma = t_{\gamma J+I+\Lambda}$ and

$$\theta_\gamma(t) = \sin^2 \frac{\pi(t-\tau_\gamma)}{2(\sigma_\gamma - \tau_\gamma)} \tag{25}$$

After the multiplication, the signal fragment is different from zero only in the middle part of the interval, therefore the next interval is chosen after receiving $J = L - 2I - \Lambda$ switching time instants, thus ensuring overlapping of the intervals. By combining all intervals, it is possible to obtain the whole reconstructed signal

$$\hat{x}(t) = \sum_{\gamma \in Z} \hat{x}_\gamma(t) w_\gamma(t), \tag{26}$$

which can futher be low pass filtered in order to reconstruct the initial signal frequency bandwidth before it was multiplied by the window function.

V. Simulation results

The dynamic power consumption of the trigger is directly proportional to the switching activity [9]. It means that the energy consumption of the whole ASDM circuit reduces, if the average switching rate of the Schmitt trigger decreases.

This leads also to a decreased number of time codes needed to be transmitted.

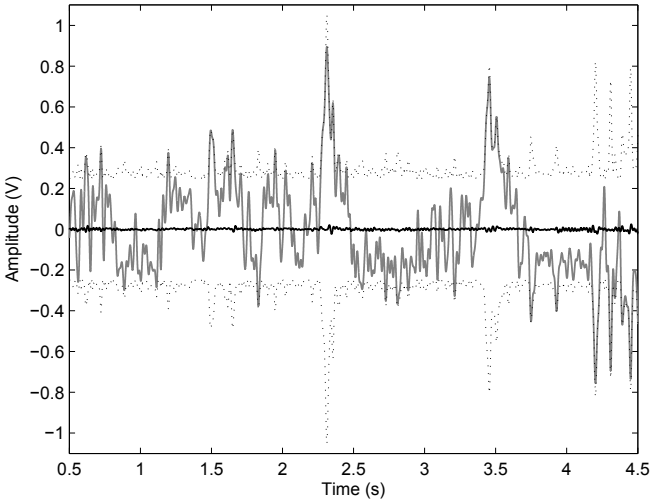

Fig. 3. Original signal $x(t)$ (gray solid line); error signal $x(t) - \hat{x}(t)$ (black solid line) after reconstruction; positive and negative envelopes $c(t)$ and $-c(t)$ (dotted lines) of $x(t)$.

The non-adaptive ASDM and adaptive AA-ASDM were tested on up to 49 Hz bandlimited EEG signals. One example of such a test signal $x(t)$ and its envelope function $c(t) = 0.25 + x^2(t)$ is shown in Fig.3.

The average amounts of triggering events per second for different $\alpha = \beta$ values are shown in Table 1. In both cases the obtained maximum distance between consecutive trigger times was close and did not exceed the Nyquist step π/Ω. The energy saving in case of AA-ASDM in comparison to ASDM was calculated as

$$E = (1 - \frac{N_{\text{AA-ASDM}}}{N_{\text{ASDM}}}) \cdot 100\%. \tag{27}$$

Table 1 : Comparison of ASDM and AA-ASDM

$\alpha = \beta$	N_{ASDM}	$N_{\text{AA-ASDM}}$	Energy saving, %
0.1	990	283	71.4
0.3	404	171	57.7
0.7	231	134	42.0
1	192	124	35.4
1.3	171	119	30.4
1.9	148	113	23.7
2.5	136	109	19.9

As it follows from the table, AA-ASDM is more energy efficient than ASDM at low $\alpha = \beta$ values, however, too low α and β are not recommended since high switching rates are obtained. The optimal choice could be $\alpha = \beta = 1$, when the minimum distance between consecutive trigger times in both cases is $T/3$.

After obtaining the output sequence $\{t_k\}_{k=1,2,\ldots,K}$ of AA-ASDM, the original signal $x(t)$ is reconstructed from the given

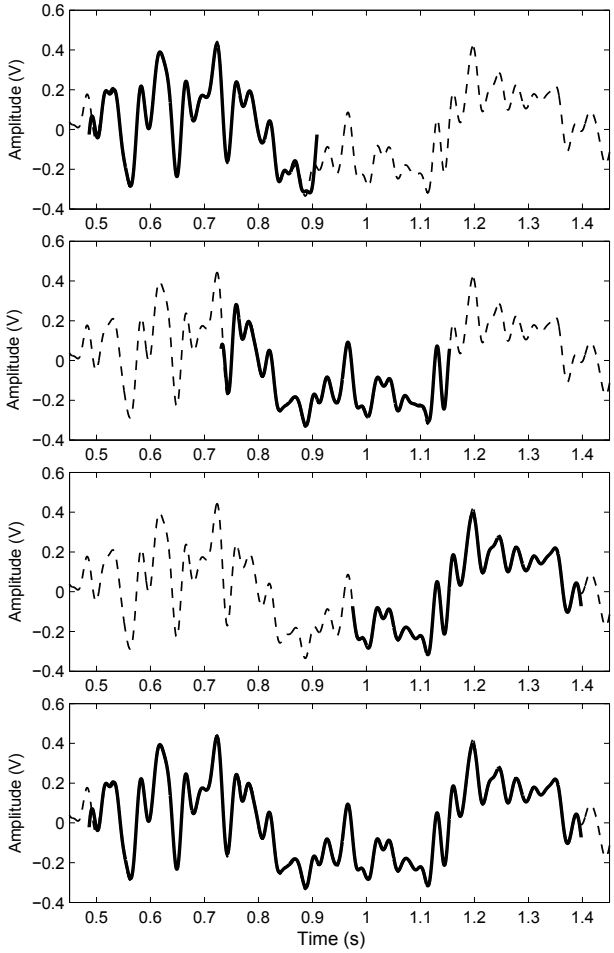

Fig. 4. Consecutive signal reconstruction: the upper three figures correspond to three consecutive signal fragments (dashed line – original signal, solid line – reconstructed signal), the lower figure corresponds to the reconstructed signal by combining all three upper fragments.

time codes as descibed in Section IV. For real-time recovery, the number L of consecutive triggerings per signal fragment was chosen to be $L = 50$, while the parameters I and Λ of the window function were chosen to be $I = 6$ and $\Lambda = 10$. In this case, after receiving every new $J = L - 2I - \Lambda = 28$ switching time instants in at least $JT/3 = 0.095$ seconds, every new signal fragment was reconstructed. It was accomplished in less than 0.09 seconds confirming that real-time signal recovery is possible. The reconstructed three fragments and their combined signal are shown in Fig.4, while the error signal $x(t) - \hat{x}(t)$, which is the difference between the original signal $x(t)$ and the recontructed combined signal $\hat{x}(t)$, of more longer duration is shown in Fig.3 by the black solid line.

VI. Conclusions

In this paper it is shown that it is possible to considerably reduce the switching activity of ASDM, if the classical circuit of ASDM is supplemented with the time-varying envelope function of the input signal in the feedback loop of the circuit. Since the maximum distance between consecutive

trigger times does not exceed the Nyquist step, it is still possible to reconstruct the signal from the obtained reduced time sequence.

For different $\alpha = \beta$ values, it is possible to achieve up to 71% energy saving compared to non-adaptive ASDM. As the $\alpha = \beta$ values grow, the advantage (in switching activity) of amplitude adaptive ASDM over non-adaptive ASDM becomes less, however, it is not recommended to choose too high these values since the variance of distances between consecutive trigger times reduces and more precision (more bits) is needed to measure the distances. Too low $\alpha = \beta$ values are not recommended as well since high switching activity appears in both cases.

ACKNOWLEDGMENT

This work is supported by the Latvian National research program SOPHIS under grant agreement Nr.10-4/VPP-4/11.

REFERENCES

[1] Marc Renaudin, "Asynchronous circuits and systems: a promising design alternative," *Microelectronic engineering*, vol. 54, no. 1, pp. 133–149, 2000.

[2] Tomislav Matic, Tomislav Svedek, and Marijan Herceg, "Limit cycle frequency jittering of an asynchronous sigma-delta modulator," in *Telecommunication in Modern Satellite, Cable, and Broadcasting Services, 2009. TELSIKS'09. 9th International Conference on*. IEEE, 2009, pp. 198–201.

[3] David Kinniment, Alex Yakovlev, and Bo Gao, "Synchronous and asynchronous ad conversion," *Very Large Scale Integration (VLSI) Systems, IEEE Transactions on*, vol. 8, no. 2, pp. 217–220, 2000.

[4] Luís HC Ferreira and Sameer R Sonkusale, "A 0.25-v 28-nw 58-db dynamic range asynchronous delta sigma modulator in 130-nm digital cmos process," .

[5] CJ Kikkert and DJ Miller, "Asynchronous delta sigma modulation," in *Proc. IREE*, 1975, vol. 36, pp. 83–88.

[6] K Ozols, Rolands Shavelis, and Modris Greitans, "Amplitude adaptive asynchronous sigma-delta modulator," in *Image and Signal Processing and Analysis (ISPA), 2013 8th International Symposium on*. IEEE, 2013, pp. 467–470.

[7] Aurel A Lazar, László T Tóth, et al., "Time encoding and perfect recovery of bandlimited signals.," in *ICASSP (6)*, 2003, pp. 709–712.

[8] Aurel A Lazar, Erno K Simonyi, and László T Tóth, "A real-time algorithm for time decoding machines," in *Signal Processing Conference, 2006 14th European*. IEEE, 2006, pp. 1–5.

[9] Binu K Mathew, "The perception processor," *Ph.D. thesis*. The University of Utah, 2004.